Surface-State Bipolaron Formation on a Triangular Lattice in thesp-TypeAlkali-Metal/Si(111)Mott Insulator

Luis Alfonso Cardenas Arellano, Yannick Fagot-Revurat, Luc Moreau, Bertrand Kierren, Daniel Malterre

Surface-State Bipolaron Formation on a Triangular Lattice in the *sp*-Type Alkali-Metal/Si(111) Mott Insulator

L. A. Cardenas, Y. Fagot-Revurat, L. Moreau, B. Kierren, and D. Malterre

Institut Jean Lamour, UMR 7198, Nancy Université/CNRS, B.P. 239 F-54506 Vandœuvre-lès-Nancy, France

(Received 17 February 2009; published 21 July 2009)

We report on new low-energy electron diffraction, scanning tunneling microscopy, and angle-resolved photoemission spectroscopy studies of alkali-metal/Si(111) previously established as having a Mott-insulating ground state at surface. The observation of a strong temperature dependent Franck-Condon broadening of the surface band together with the novel $\sqrt{3} \times \sqrt{3} \rightarrow 2(\sqrt{3} \times \sqrt{3})$ charge and lattice ordering below 270 K evidence a surface charge density wave in the strong electron-phonon coupling limit ($g \approx 8$). Both the adiabatic ratio $\hbar\omega_0/t \approx 0.8$ and the effective pairing energy $V_{\mathrm{eff}} = U - 2g\hbar\omega_0 \approx -800$ meV are consistent with the possible formation of a bipolaronic insulating phase consisting of alternating doubly occupied and unoccupied dangling bonds as expected in the Holstein-Hubbard model.

DOI: 10.1103/PhysRevLett.103.046804 PACS numbers: 73.20.At, 71.27.+a, 71.38.Mx, 79.60.−i

The question of the relevance of electron-phonon coupling (EPC) in the physical properties of strongly correlated systems has been recently addressed for various materials like manganites [1], alkali-metal-doped C_{60} [2], vanadium oxides [3] and especially cuprates for which the interplay between charge, spin and lattice degrees of freedom is still unsolved [4]. From the theoretical point of view, the half-filled Holstein-Hubbard model, including both electron-electron and electron-phonon coupling, has been intensively studied [5–9]. In the weak-coupling limit, a correlated or polaronic metal occurs. In the strong-coupling limit, the competition between electronic and lattice effects leads to an effective interaction $V_{\mathrm{eff}} = U - 2g\hbar\omega_0$ whose sign determines the ground state: a Mott-Hubbard insulating one (MHI) takes place at large U whereas an attractive *e-e* interaction can occur for large g resulting in a quantum phase transition from a MHI to a bipolaronic insulating phase (BPI). Therefore, localized electron pairs are trapped by their self-induced lattice deformation leading to the formation of a charge density wave state implying a doubling of the lattice parameters [10] as early observed in 3D titanium oxides [11]. Lowering the dimension, itinerant small bipolarons on triangular lattices have been recently predicted to form a Bose-Einstein condensate giving possibly rise to high temperature superconductivity [12].

Peculiar Mott insulators implying *sp* states can be found at semiconducting surfaces. Indeed, the reduction of the bandwidth W and of screening effects at surface have been first proposed to explain the Mott transition leading to the insulating properties of K/Si:B [13,14]. Then, such a Mott state has been identified as a generic property of semiconducting surfaces with dangling bonds (DB) organized in a $\sqrt{3} \times \sqrt{3}$-surface reconstruction, i.e., presenting a triangular pattern [15], such as SiC(0001) [16] and C/Si(111) [17]. Recently, surface science tools have been used to solve the metal-insulator transition in Sn/Ge(111) [18,19] and Sn/Si(111) [20]. This triangular topology has been predicted to induce exotic magnetic phases [13,16,21] and even superconductivity upon doping [22]. Otherwise, weak EPC theories have been proposed to explain several surface reconstructions as well as ARPES and STS spectral features [23–25]. Weitering and co-workers have pointed out the possible role of EPC in the case of K/Si:B [13]. Angle-resolved photoemission spectroscopy (ARPES), low-energy electron diffraction (LEED) and scanning tunneling microscopy (STM) have been combined to solve the fundamental nature of the K/Si:B interface. Indeed, the novel $2(\sqrt{3} \times \sqrt{3})$ insulating phase observed here together with the evidence of a phonon-dressed spectral function allow us to identify the ground state of K/Si:B as a bipolaronic insulator rather than a Mott-Hubbard one. Our results imply that K/Si:B is, to our knowledge, the first experimental realization of a BPI phase on a triangular lattice showing that *in fine* the EPC drives the electronic properties in this correlated material.

Boron-enriched Si(111) substrates ($\rho \approx 10^{-3}\ \Omega\,\mathrm{cm}$) have been shortly annealed at 1450 K followed by a few hours heating at 1000 K to favor the segregation of B atoms in the pentavalent S_5 subsurface site [26]. A nearly free of defects $\sqrt{3} \times \sqrt{3}R30$ surface reconstruction ($a' = 6.66$ Å) with less than 0.015 B vacancies per nm^2 has been usually obtained as checked by STM. On the Si(111) surface, the dangling bonds are reorganized in a 7×7 surface reconstruction with a weakly dispersive adatom half-filled surface state ensuring its slight metallic character [23]. At the opposite, the B-enriched Si(111) substrate exhibits a semiconducting behavior: DB electrons are trapped by boron impurities leaving an empty surface state [27]. The B-enriched Si(111) band structure has been shown to be well described by *ab initio* calculations [28]. The K/Si:B interface was prepared at 300 K by evaporation of K atoms from a SAES getter with a deposition rate of 0.13 monolayer/min in a vacuum better than 5×10^{-10} mbar. The room-temperature (RT) saturation coverage, defined as 1 K atom per reconstructed unit cell (1/3 of

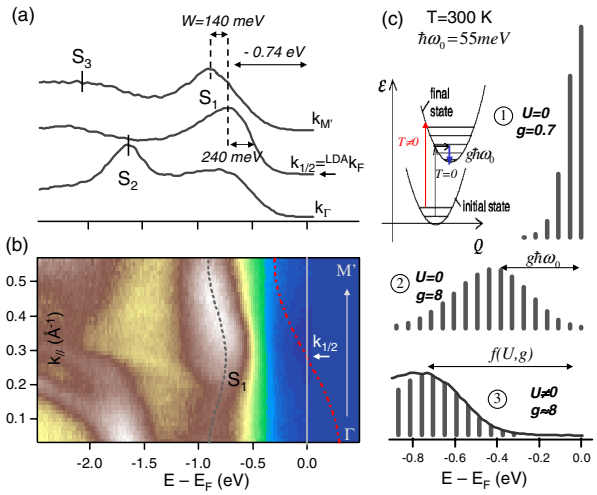

FIG. 1 (color online). EDC's (a) and ARPES intensity map (b) measured along Γ–M' in 0.33 ML K/Si:B at 300 K; red and black lines materialize, respectively, the tight-binding and the experimental dispersion curves; (c) Franck-Condon spectral function and adjustment of the experimental leading edge of the $k = k_{1/2}$ spectra (continuous black line).

alkali-metal monolayer) has been identified by *in situ* monitoring of Auger Si, B, and K lines. According to previous studies, the room-temperature sticking coefficient falls down after the completion of the first layer, i.e., at the saturation coverage of 0.33 ML K/Si:B [29]. The LEED pattern obtained at saturation indicates a well-defined $\sqrt{3} \times \sqrt{3}R30$ surface reconstruction in agreement with the K chemisorption in the highly coordinated H_3 site [28]. Previous studies of core-levels have established a charge transfer occurring from the K 4*s* orbital to the silicon ad-atom at surface, leading to a new DB state induced by K adsorption [30]. Naively, with one electron per DB-orbitals, a half-filled metallic state was expected to be formed on a triangular lattice as shown by *ab initio* calculations [28].

ARPES intensity map and energy dispersion curves (EDC) obtained at the saturation coverage with an energy and momentum resolution of 10 meV and 0.04 Å^{-1} are displayed in Fig. 1. According to previous results [29], a well-defined K-induced surface state labeled S_1 is developed in the semiconducting gap, its spectral weight being related to the amount of K deposited. The S_2 and S_3 bands have been ascribed to rest-atom and backbond surface states [28]. As a new insight, the surface-state dispersion has been accurately measured along the Γ–M' (Γ–K') high symmetry direction of the $\sqrt{3} \times \sqrt{3}$-hexagonal SBZ. In qualitative agreement with calculations, the surface band dispersion presents minima at M' ($k = 0.55$ Å^{-1}, $E - E_F = -880$ meV) and K' ($k = 0.63$ Å^{-1}, $E - E_F = -900$ meV) with a positive effective mass. Nevertheless, contrary to the tight-binding predictions [dashed-dotted line in Fig. 1(b)] or *ab initio* calculations [28]), a clear band folding occurs close to half of the BZ ($k = k_{1/2} \approx 0.27$ Å$^{-1} \approx k_F^{\mathrm{LDA}}$) leading to a second minimum in the band dispersion at the zone center (Γ) and the opening of a gap larger than 500 meV. A similar behavior has been observed along Γ–K' leading to the reduction by a factor of 4 of the RT apparent surface BZ. However, the spectral weight is mainly located in the unfolded part of the one-electron surface band ($k > k_{1/2}$). In addition, a strongly renormalized experimental bandwidth $W_{\mathrm{expt}}^{\mathrm{occ.}} = 140$ meV have been deduced compare to the *ab initio* value of 300 meV expected for the occupied part [28]. This large gap has been first interpreted as resulting from a correlation induced metal-insulator transition [13]. Indeed, the Harrison criterion $U/W \gg 1$ was supposed to be full-filled at surface for DB electrons with $U \approx 1.5$ eV [13] and $W_{\mathrm{LDA}}^{\mathrm{full}} \approx 0.6$ eV ($t \approx 0.07$ eV) [28] giving rise to a surface-induced Mott transition [14]. The binding energy $E_B^{S1} = 0.75$ eV $\approx U/2$ agrees well with the Mott-insulator model. K/Si:B was claimed to be the first 2D Mott-Hubbard material based on *sp*-band, the triangular topology being speculated to give rise to singular magnetic properties [13,21].

The novel apparent band folding at $k_F^{\mathrm{LDA}} \approx k_{1/2}$ evidenced here does not contradict the MI model [7]. Nevertheless, one should remark on Fig. 1(a) the strong intrinsic broadening of the SS at 300 K even considerably larger than the bandwidth. Weitering and co-workers have initially proposed to interpret this broadening as a possible Franck-Condon (FC) envelop due to a strong EPC but did not prove it [13]. For localized electrons, the FC model describes the coupling of an electron to a single harmonic oscillator [31] as depicted in Fig. 1(c) for the specific case of K:SiB at 300 K. As a general feature of EPC, the PES spectra contain phonon side bands at $E_k = E_k^0 - n\hbar\omega_0$ ($n = 0, 1, \ldots$) reflecting the screening of the photo hole by localized vibrational excitations [31]. The $T = 0$ intensity of the nth transition is therefore given by the FC factor $I(n) = g^n \exp(-g)/n!$, g characterizing the strength of the EPC. In the weak-coupling limit $g < 1$, the zero-phonon transition, at the free binding energy $E_k = E_k^0$, is the most pronounced, other transition causes a broadening of the PES line [case 1, Fig. 1(c)]. In the strong-coupling limit $g > 1$, the spectral weight is redistributed over a wide energy range with a maximum at $E_k = E_k^0 - g\hbar\omega_0$ [case 2, Fig. 1(c)]. Additional extrinsic broadening usually prevents the clear observation of multiphonon side bands [25]. Therefore, for $g \gg 1$, a nearly-Gaussian incoherent broad spectral intensity is experimentally observed whose width is determined by the average number of phonons involved in the final state at $T = 0$. Moreover, at finite temperature ($k_B T \geq \hbar\omega_0$), the line shape is broadened due to the contribution of excited vibrationnal levels [31]. This has been commonly used as a fingerprint for the EPC signature even in strongly correlated materials [32]. Assuming the FC broadening as the dominant contribution to the experimental spectral width, an attempt has been made to adjust HWHM of the low-energy tail of the room-temperature

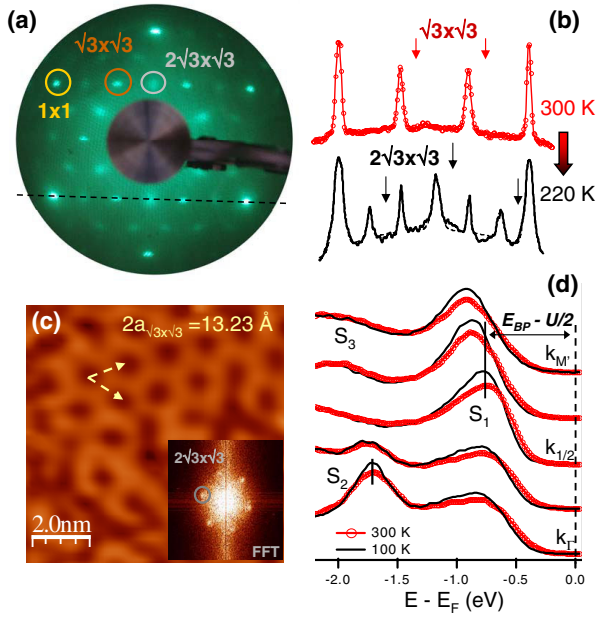

FIG. 2 (color online). (a) LEED pattern obtained at 220 K, (b) profiles obtained at 300 and 220 K; (c) STM image ($V = 1.3$ V, $I = 0.2$ nA) obtained at 80 K; inset: FFT obtained on a 80 nm $\times$ 80 nm image; (d) ARPES spectra obtained at 300 and 100 K.

$k = k_{1/2}$ EDC [case 3, Fig. 1(c)]. A large coupling constant $g \approx 8$ and a phonon energy $\hbar\omega_0 = 55$ meV have been deduced consistent with those obtained on similar semiconducting surfaces [23,25]. Such a strong EPC might possibly drive surface reconstructions as presented in the following.

On one hand, the LEED pattern obtained at 220 K displayed in Fig. 2(a) exhibits a novel $2(\sqrt{3} \times \sqrt{3})$ phase at surface. Corresponding profiles obtained at 300 and 220 K presented in Fig. 2(b) indicate a clear phase transition involving a lattice distortion, i.e., a doubling of the hexagonal lattice parameters. The narrow 220 K-diffraction peaks indicate that the new structural ordering corresponds to a well established long-range ordered phase. The transition has been identified around $T_c \approx 270$ K. However, the long-range ordering, the transition temperature, and a moderate hysteretic behavior depend on the amount of Boron vacancies at surface acting as defects. A more detailed study will be presented elsewhere. In addition to the lattice distortion, a clear charge density modulation is evidenced by our STM study of the low-T phase presented in Fig. 2(c). Despite a small disorder, the 2D-FFT spectrum obtained on a 80×80 nm^2 STM image exhibits a well-defined $2(\sqrt{3} \times \sqrt{3})$ peaks evidencing the quadrupling of the unit cell at surface. On the other hand, quantitative modifications of the surface band have been observed as illustrated in Fig. 2(d). A systematic redistribution of spectral weight to higher binding energies is clearly evidenced including a $\delta E \approx 60$ meV shift of the SS leading edge between 300 and 200 K, this one remaining constant below 200 K [see also in Fig. 3(a)]. As evidenced in Fig. 2(d), other bands remain unaffected down to 100 K, indicating there are not charge or photovoltage effects and ensuring that only the K-induced surface state is involved in this surface transition. The bandwidth is slightly reduced together with a stabilization of the electronic surface band in agreement with a more insulating LT phase. Moreover, we would like to point out the clear narrowing of the intrinsic width of the surface band over a wide temperature range, even far from the transition. Indeed, following the procedure of Shen and co-workers [32], a Gaussian adjustment of the HWHM (the low-energy tail) of the $k = k_{1/2}$ ARPES spectra have been made for 100, 200, and 300 K as presented in Fig. 3(a). The result has been displayed as function of the temperature in Fig. 3(b) and compared with those we have calculated from the FC model varying g, $\hbar\omega_0$ and taking into account the temperature. Again, a good agreement between experimental data and calculations is achieved for $g \approx 8$ and $\hbar\omega_0 \approx 55$ meV. Therefore, the novel set of data presented in this letter strongly supports the existence of a $\sqrt{3} \times \sqrt{3} \rightarrow 2(\sqrt{3} \times \sqrt{3})$ insulating to insulating surface phase transition involving a lattice dimerization, a charge modulation and a net energy gain for surface-state electrons. Contrary to previous studies, they shed on light the strong relevance of the electron-phonon coupling to understand the K/Si:B ground state.

The absence of Fermi surface, the large gap measured in both phases and the reconstructed LT-phase contradict previous *ab initio* predictions [28]. Therefore, g and U are supposed to possibly play a role and the data have been analyzed in the framework of the Hostein-Hubbard model at half-filling whose generic $T = 0$ phase diagram is depicted in Fig. 3(c) (taken from DMFT calculations [8]). On one hand, a Mott state is achieved for $U/W \geq 1.6$ but does not imply a lattice symmetry breaking. However, it

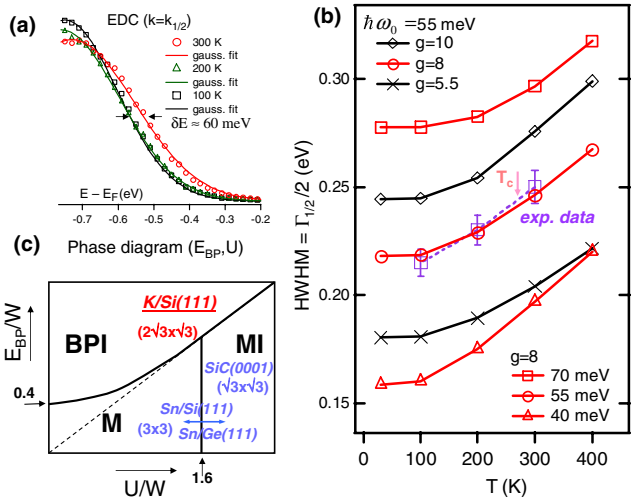

FIG. 3 (color online). EDC's($k = k_{1/2}$ (a), calculated FC broadening compared to the experimental Gaussian fits (b); general (g, U) phase diagram in the Holstein-Hubbard model [8] (c).

can be favored by a lattice reconstruction ($3 \times 3 \rightarrow \sqrt{3} \times \sqrt{3}$ in Sn/Ge(111) [18]) or by a precursive CDW transition as observed for $1T$-$TaSe_2$ [33]. On the other hand, in the Holstein model ($U = 0$), a soft phonon induces a lattice instability beyond a critical e-ph coupling leading to the formation of a CDW state involving an increase in the unit cell in qualitative agreement with our experimental data [6–8]. A high g and an adiabatic ratio close to 1 suggest the strong e-ph coupling limit is reached here leading to the formation of a bipolaronic insulator (BPI). Indeed, the pairing energy defined by $E_{\mathrm{BP}} = 2g\hbar\omega_0$ full-filled the criterion $E_{\mathrm{BP}}/W = 1.2 > 0.4$ for establishing the BPI phase [8]. Assuming the $4s$ alkali-metal electron is mainly transferred to the DB orbital (Si ad-atom) [29], the quadrupling of the unit cell is easily obtained by alternating doubly- and unoccupied DB site as expected for the BPI state [7,10]. As for BCS theory of superconductivity, the full gap corresponds in this case to twice the pairing energy for bounded two electrons [6]. Therefore, the occupied part of the gap is theoretically expected to be $E_{\mathrm{BP}} \approx 880$ meV [6]. However, the effective pairing energy might be reduced by U leading to an occupied gap given by $E_{\mathrm{BP}} - U/2$. Hence, a weak $U \approx 160$ meV might explained our LT-experimental gap of less than 800 meV. The BPI phase is predicted to present a poorly dispersive backfolded phonon-dressed ARPES spectral function [7,10] in agreement with the results presented in this Letter. Therefore, as suggested in the phase diagram presented in Fig. 3(c), the BPI ground state might be reached in 0.33 ML K/Si(111)-B contrary to other $\sqrt{3}$-semiconducting surfaces. Such a BPI phase has been also proposed to describe the ground state of 0.25 ML Na/GaAs(110) on the basis of DFT calculations [34]. This suggests the BPI ground state as a common property of ultrathin alkali-metal layer deposited on semiconducting substrates. Unlike weak-coupling theories, Fermi surface nesting properties are not necessary to reach the long-range ordered state in the strong-coupling limit [10]. Hence, the high temperature phase might not be necessary metallic. Indeed, a precursive short range ordered intermediate insulating phase, defined as a bipolaronic liquid, has been observed a long time ago in Ti_4O_7 [11], the long-range Ti^{3+}-Ti^{4+} charge ordering occurring only below 130 K. The precursive diffusive background observed in LEED patterns together with the well established surface-state band folding above T_c, could be indications for a short-range ordered BPI phase at 300 K, the lifetime characterizing polaronic excitations being short enough to experiment the fluctuating surface reconstruction. This is an open question. Because of their bounded nature, bipolarons should carry a singlet spin state making these surfaces nonmagnetic contrary to previous speculations [13].

Substitution with other alkali-metal atoms should provide a way to explore the (g, U) phase diagram of the 2D Holstein-Hubbard model on a triangular lattice. Many interesting aspects such as isotopic effects, core level signature of the charge ordering, direct measurements of the typical phonon energy by EELS should be investigated in the future. Finally, theoretical and experimental works carried on these SC surfaces these last ten years have evidenced their extreme proximity with the Mott-Hubbard physics in presence of a coupling to the lattice [22]. Doping these half-filled systems could provide the opportunity to investigate novel ground state at surface including high-T_c superconductivity.

We gratefully acknowledge to A. E. Trumper, L. O. Manuel, F. Flores, J. Ortega, C. Tournier-Colleta, and A. Tejeda for our stimulating discussions.

[1] A. J. Millis, Nature (London) **392**, 147 (1998).
[2] O. Gunnarson, Rev. Mod. Phys. **69**, 575 (1997).
[3] P. Limelette *et al.*, Science **302**, 89 (2003).
[4] G. H. Gweon *et al.*, Nature (London) **430**, 187 (2004).
[5] E. Berger, P. Valasek, and W. Von Der Linden, Phys. Rev. B **52**, 4806 (1995).
[6] D. Meyer and A. C. Hewson, Phys. Rev. Lett. **89**, 196401 (2002).
[7] H. Fehske *et al.*, Phys. Rev. B **69**, 165115 (2004).
[8] G. S. Jeon *et al.*, Phys. Rev. B **70**, 125114 (2004).
[9] G. Sangiovanni *et al.*, Phys. Rev. Lett. **94**, 026401 (2005).
[10] U. Gobel, A. S. Alexandrov, and H. Capellmann, Z. Phys. B **96**, 47 (1994), and references therein.
[11] S. Lakkis *et al.*, Phys. Rev. B **14**, 1429 (1976).
[12] J. P. Hague *et al.*, Phys. Rev. Lett. **98**, 037002 (2007).
[13] H. H. Weitering *et al.*, Phys. Rev. Lett. **78**, 1331 (1997).
[14] C. S. Hellberg and S. C. Erwin, Phys. Rev. Lett. **83**, 1003 (1999).
[15] F. Flores, J. Ortega, and R. Perez, Surf. Sci. Lett. **6**, 411 (1999).
[16] G. Santoro, S. Scandolo, and E. Tossati, Phys. Rev. B **59**, 1891 (1999).
[17] G. Profeta and E. Tossati, Phys. Rev. Lett. **95**, 206801 (2005).
[18] R. Cortes *et al.*, Phys. Rev. Lett. **96**, 126103 (2006).
[19] S. Colonna *et al.*, Phys. Rev. Lett. **101**, 186102 (2008).
[20] S. Modesti *et al.*, Phys. Rev. Lett. **98**, 126401 (2007).
[21] A. E. Trumper, C. Gazza, and L. O. Manuel, Phys. Rev. B **69**, 184407 (2004).
[22] G. Profeta and E. Tossati, Phys. Rev. Lett. **98**, 086401 (2007).
[23] I. Barke *et al.*, Phys. Rev. Lett. **96**, 216801 (2006).
[24] C. Gonzalez *et al.*, Phys. Rev. Lett. **96**, 136101 (2006).
[25] M. Brethe *et al.*, Phys. Rev. Lett. **97**, 206801 (2006).
[26] P. Baumgartel *et al.*, Phys. Rev. B **59**, 13 014 (1999).
[27] T. M. Grehk *et al.*, Phys. Rev. B **46**, 2357 (1992).
[28] H. Q. Shi, M. W. Radny, and P. V. Smith, Phys. Rev. B **70**, 235325 (2004).
[29] H. H. Weitering *et al.*, Phys. Rev. B **48**, 8119 (1993).
[30] Y. Ma *et al.*, Phys. Rev. Lett. **65**, 2173 (1990).
[31] G. D. Mahan, *Many-Particles Physics* (Plenum, New York, 1981).
[32] K. M. Shen *et al.*, Phys. Rev. B **75**, 075115 (2007).
[33] L. Perfetti *et al.*, Phys. Rev. Lett. **90**, 166401 (2003).
[34] O. Pankratov and M. Scheffler, Phys. Rev. Lett. **71**, 2797 (1993).